Inflammasome-dependent IL-1β release depends upon membrane permeabilisation

Fatima Martín-Sánchez[1]*, Catherine Diamond[2,3]*, Marcel Zeitler[5], Ana Gomez-Sanchez[1], Alberto Baroja-Mazo[1], James Bagnall[2], David Spiller[2], Michael White[2], Michael J. D. Daniels[2], Alessandra Mortellaro[3], Marcos Peñalver[4], Pawel Paszek[2], Julia P. Steringer[5], Walter Nickel[5], David Brough[2,+], Pablo Pelegrín[1,2,+]

[1]Grupo de Inflamación Molecular, Centro de Investigación Biomédica en Red en el Área Temática de Enfermedades Hepáticas y Digestivas, Hospital Clínico Universitario Virgen de la Arrixaca, Instituto Murciano de Investigación Biosanitaria-Arrixaca, 30120 Murcia, Spain

[2]Faculty of Life Sciences, University of Manchester, Manchester M13 9PT, United Kingdom

[3]Singapore Immunology Network (SIgN), Agency for Science Technology and Research (A*STAR), Singapore 138648

[4]Probelte Biotechnology, S.L., Murcia, Spain

[5]Heidelberg University Biochemistry Center, 69120 Heidelberg, Germany

*Equal contribution

[+]Share last authorship, corresponding author

Contacts: Dr. Pablo Pelegrín, Tel: +34868885038; e-mail: pablo.pelegrin@ffis.es. Dr. David Brough, Tel: +441612755039; email: david.brough@manchester.ac.uk

Running Title: IL-1β release via membrane permeabilisation.

Abstract

Interleukin (IL)-1β is a critical regulator of the inflammatory response. IL-1β is not secreted through the conventional ER-Golgi route of protein secretion and to-date its mechanism of release has been unknown. Crucially its secretion depends upon the processing of a precursor form following the activation of the multi-molecular inflammasome complex. Using a novel and reversible pharmacological inhibitor of the IL-1β release process, in combination with biochemical, biophysical and real-time single-cell confocal microscopy with macrophage cells expressing Venus labelled IL-1β, we have discovered that the secretion of IL-1β after inflammasome activation requires membrane permeabilisation, and occurs in parallel with the death of the secreting cell. Thus in macrophages the release of IL-1β in response to inflammasome activation appears to be a secretory process independent of non-specific leakage of proteins during cell death. The mechanism of membrane permeabilisation leading to IL-1β release is distinct from the unconventional secretory mechanism employed by its structural homologues FGF2 or IL-1α, a process that involves the formation of membrane pores but does not result in cell death. These discoveries reveal key processes at the initiation of an inflammatory response and deliver new insights into mechanisms of protein release.

Abbreviations: AIM2, Absent in melanoma 2; ASC, Apoptosis-associated speck-like protein containing a caspase recruitment domain; BRET, Bioluminescence resonance energy transfer; DAMPs, Damage associated molecular patterns; FGF2, Fibroblast growth factor 2; IL-1β, Interleukin-1beta; LDH, Lactate dehydrogenase; LPS, Lipopolysaccharide; NLR, Nucleotide-binding domain and Leucine-rich repeat containing Receptor; NLRP3, NACHT; LRR and PYD domains-containing protein 3; PAMPs, Pathogen associated molecular patterns; PRRs, Pattern recognition receptors; PI, Propidium iodide; WT, Wild-type.

Introduction

Interleukin-1β (IL-1β) is a pro-inflammatory cytokine which is central for host responses to infection[1]. IL-1β is produced as an inactive precursor called pro-IL-1β mainly by inflammatory cells of myeloid lineage. Pro-IL-1β is rapidly induced upon exposure of inflammatory cells to pathogen associated molecular patterns (PAMPs) or damage associated molecular patterns (DAMPs), that bind to pattern recognition receptors (PRRs) to upregulate pro-inflammatory gene expression[2]. A cell expressing pro-IL-1β is suggested to be 'primed' and in order for the secretion of active mature IL-1β molecules the primed cell must encounter an additional PAMP or DAMP stimulation (signal 2) to activate cytosolic PRRs, often of the Nucleotide-binding domain and Leucine-rich repeat containing Receptor (NLR) family, to form large multi-protein complexes called inflammasomes[3]. The best characterised inflammasome is formed by the PRR NLRP3[4]. Inflammasomes are composed of the PRR, pro-caspase-1, and an adaptor protein called ASC (apoptosis-associated speck-like protein containing a caspase recruitment domain), that interact via homology binding domains[3]. Following activation inflammasomes cause the activation of caspase-1 and the processing of pro-IL-1β to a mature form that is secreted.

IL-1β does not traffic through the ER or Golgi and the precise mechanisms of its secretion are poorly defined. Following a recent review of the literature we have postulated that there are a number of possible mechanisms through which IL-1β could exit the cell[5]. Potential secretory mechanisms include its release through the regulated secretion of lysosomes[6], the shedding of microvesicles from the plasma membrane[7], or its direct release across a hyper-permeable plasma membrane[8]. This last mechanism is perhaps related to cell death, which in many instances is linked to IL-1β secretion. Interestingly, another non-conventionally secreted protein, FGF2, is secreted by membrane insertion of FGF2 oligomers as intermediates in FGF2 membrane translocation as part of its secretory mechanism[9]. Despite having very little sequence homology, FGF2 and IL-1β are structural homologues with both

containing a β-barrel structure[10,11]. Thus it is possible that mature IL-1β could create membrane translocation pores in a manner analogous to FGF2 to facilitate its release.

Using the canonical inducer of NLRP3 inflammasome activation, extracellular ATP (acting *via* the P2X7 receptor), we previously reported that release of IL-1β preceded that of the cell death marker lactate dehydrogenase (LDH) from primary peritoneal macrophages[12]. However, IL-1β was secreted just before LDH was released suggesting that the cells were already committed to cell death by the time they secreted IL-1β[12]. However, it seems unlikely that IL-1β release can only be linked to cell death and IL-1β is released from human monocytes or neutrophils in the absence of cell death[13,14], suggesting that there are perhaps cell specific mechanisms of release. Here we used sensitive single-cell quantitative approaches in addition to new pharmacological interventions with membrane stabilising reagents to show that in response to NLRP3 inflammasome activation, the secretion of IL-1β from macrophages depended upon permeabilisation of the plasma membrane, occurred concomitantly with cell death, and was distinct from the specific formation of translocation pores utilised by FGF2.

Results

IL-1β does not possess FGF-2-like properties of membrane pore formation

FGF2 secretion is a specific and tightly regulated process that involves direct translocation across plasma membranes, in a process that involves $PI(4,5)P_2$-dependent membrane recruitment[15], oligomerisation[9], membrane pore formation[9,16] and is regulated by tyrosine phosphorylation of FGF2 mediated by Tec kinase[17]. Given the structural similarity between FGF2 and IL-1β, and that the secretion of IL-1β has recently been reported to potentially involve changes in plasma membrane integrity[8], we hypothesised that IL-1β may also be capable of binding to $PI(4,5)P_2$ concomitant with the formation of membrane pores. Both authentic and fluorescently labelled variants of phosphomimetic FGF2[9], pro-IL-1β and IL-1β were expressed and purified to homogeneity. In a first set of experiments, authentic variants were tested with regard to binding to $PI(4,5)P_2$-containing liposomes using classical biochemical flotation experiments (Figure 1A,B). Fraction 1 contains protein that bound to membranes, fraction L is the load of the gradient. While phosphomimetic FGF2 was found to bind efficiently to $PI(4,5)P_2$-containing liposomes, neither pro-IL-1β nor mature IL-1β bound to $PI(4,5)P_2$ to a significant extent (Figure 1A,B,C). Consistent with previous studies[9,16] these experiments revealed the formation of SDS-resistant FGF2 oligomers that form upon membrane binding. These findings could be confirmed with fluorescently labelled forms of phosphomimetic FGF2, pro-IL-1β and IL-1β using a flow cytometry setup to quantify protein-lipid interactions[18]. Similar to the flotation experiments (Figure 1A,B,C), neither pro-IL-1β nor mature IL-1β bound to membranes whereas phosphomimetic FGF2 showed strong membrane binding that was dependent on the presence of $PI(4,5)P_2$ (Figure 1D). In another set of experiments, we tested whether pro-IL-1β or mature IL-1β could permeabilize membranes *in vitro* analysing membrane passage of a small fluorescent tracer[9,19]. As shown in Figure 1E and F, a membrane permeabilising activity of these proteins could not be observed. By contrast, as reported previously, phosphomimetic FGF2 forms membrane pores in a $PI(4,5)P_2$-dependent manner resulting in membrane passage of the fluorescent

tracer. These data demonstrate that neither pro- nor mature IL-1β have properties resembling those of FGF2 regarding membrane binding and pore formation.

IL-1β release depends upon plasma membrane permeabilisation

To further interrogate the mechanisms of IL-1β release from macrophages, we transformed immortalised mouse bone marrow derived macrophages (BMDMs) with a lentiviral vector to express pro-IL-1β as a C-terminal fluorescent Venus protein fusion. In these cells the distribution of pro-IL-1βVenus was cytosolic, as previously described for endogenous pro-IL-1β[12], and was processed and released in response to LPS and ATP stimulation (Supplementary Figure 1). Furthermore, the temporal pattern of IL-1β release and membrane permeabilisation/cell death (as assessed by the release of the soluble cytosolic protein LDH that leaks from the cell during necrosis), were similar between pro-IL-1βVenus transduced cells and wild type cells (Supplementary Figure 1). Consistent with the requirement of priming for NLRP3 expression[20], IL-1β was not released without prior LPS stimulation (Supplementary Figure 1). Using these cells we used time lapse confocal microscopy to observe the secretion of IL-1β (Supplementary movies 1 and 2). LPS primed cells were incubated in the presence or absence of ATP and Venus fluorescence was continuously monitored. To simultaneously monitor membrane integrity we included the cell-impermeant nucleic acid stain propidium iodide (PI) in the cell culture medium. Following the addition of ATP there was a drop in Venus fluorescence that correlated with an increase in PI fluorescence suggesting that the release of IL-1β coincided with membrane permeabilisation (Figure 2A,B). Shown are the raw data from 4 cells identified in the movie snapshots (Figure 2B). In control cells, where no ATP was added, there was some reduction of the Venus fluorescent signal and no increase in PI fluorescence (Figure 2C, Supplementary movie 3). These data suggest that IL-1β secretion from macrophages occurs across a hyper permeable plasma membrane.

The mechanism of IL-1β release was then further interrogated using the complex polyphenolic compound punicalagin (Supplementary Figure 2A). We discovered that punicalagin prevented ATP induced IL-1β secretion, but not it's processing. Therefore after ATP treatment in the presence of punicalagin mature IL-1β was associated with macrophage cell lysates (Figure 3A). Punicalagin has a complex molecular structure, and the full intact molecular structure was required to inhibit IL-1β release, since its component parts (punicalin, ellagic acid and urolithin) had no effect on IL-1β secretion (Supplementary Figure 2A,B). Pomegranate extract (Pomanox™) with a punicalagin content of 20% was also effective at preventing mature IL-1β release from ATP treated macrophages (Supplementary Figure 2C). Additionally, punicalagin was a potent blocker of plasma membrane permeabilisation (Yo-Pro-1 uptake) in response to ATP (Figure 3B), and the half maximal inhibitory concentration (IC_{50}) for IL-1β release and membrane permeabilisation were 3.91 and 7.65 μM respectively (Figure 3C). Punicalagin-mediated preservation of plasma membrane integrity was also evident measuring Yo-Pro-1 uptake after cell treatment with detergents (Figure 3D) and measuring the release of LDH to the cell supernatant following ATP treatment or detergent application (Figure 3E). Punicalagin was able to maintain the integrity of macrophages treated with detergents (Supplementary Figure 3A), although this protection was overcome as the dose of detergent applied was increased (Supplementary Figure 3B). As further controls, punicalagin did not quench Yo-Pro-1 fluorescence, nor did it directly inhibit LDH enzyme activity (Supplementary Figure 3C,D). The IC_{50} of punicalagin against ATP-induced LDH release was 3.67 μM, and therefore very similar to the IC_{50} for blocking IL-1β release (Figure 3F). Punicalagin treatment of immortalized macrophages expressing pro-IL-1βVenus was able to maintain cell integrity and retain fluorescence leaking from the cell after ATP application (Figure 3G and supplementary figure 3E and movies 4 and 5).

Loss of membrane integrity is not required for inflammasome formation

We then studied IL-1β secretion in response to different NLRP3 inducers and also in response to AIM2 inflammasome activation. We used an ELISA with higher sensitivity for mature IL-1β than for pro-IL-1β, and validated it comparing western blot data from LPS-primed macrophage cell lysates treated with or without ATP and punicalagin (Supplementary Figure 4A). This ELISA detected more IL-1β in lysates with mature IL-1β, than in lysates with just pro-IL-1β. Using this ELISA approach, we found that punicalagin blocked IL-1β release in response to different NLRP3 inflammasome and AIM2 activators, and mature IL-1β was retained in the cell lysate after activation of macrophages with nigericin, hypotonicity, uric acid crystals, the pore-forming toxin melittin, and dsDNA (Figure 4A). Similarly, punicalagin significantly reduced release of LDH in response to different NLRP3 and AIM2 inflammasome activators (Figure 4B). Punicalagin did not affect the cellular volume changes of macrophages in response to hypotonicity (Supplementary Figure 4B), suggesting that it was not acting as an external osmolyte to resist osmotic swelling and cell lysis. Therefore, a change in plasma membrane permeability emerges as a common mechanism for the unconventional release of IL-1β from macrophages. Punicalagin also inhibited the release of IL-1β from neutrophils, a cell type that releases IL-1β independently of cell death (Figure 4C). Furthermore, punicalagin inhibited necroptotic cell death, but not the unconventional release of IL-1α which we previously reported in response to necroptotic stimuli[21] (Figure 4D). The specificity of the effect of punicalagin to IL-1β release was further demonstrated by its failure to inhibit the conventional release of TNF-α and IL-6 (Figure 4E).

Punicalagin did not directly block P2X7 receptor activation, as assayed by increase of cytosolic Ca^{2+} or decrease of intracellular K^{+} (Figure 5A,B), cations that directly permeate through the P2X7 receptor ion channel[22]. Punicalagin did not directly interfere with NLRP3 activation as measured by BRET (Figure 5C), nor did it impair the formation of ASC specks (Figure 5D). Also, punicalagin did not inhibit caspase-1 activity after NLRP3 inflammasome

activation (Figure 5E,F), but it completely prevented release of active caspase-1 (p10 subunit), ASC and NLRP3 inflammasome components (Figure 5E).

To investigate the role of the inflammasome on plasma membrane destabilisation and cell death, we used macrophages deficient in NLRP3, ASC or caspase-1 primed with LPS and then treated with ATP. These macrophages also presented membrane permeabilisation when compared to wild type macrophages, but LDH release was abolished (Supplementary Figure 4C,D). Punicalagin was able to block plasma membrane permeabilisation in both wild type and inflammasome deficient macrophages (Supplementary Figure 4C,D).

Pharmacological and kinetic characterisation of IL-1β release

After washing punicalagin from macrophages treated with ATP, IL-1β and the p10 fragment of caspase-1 were released without the requirement of additional ATP stimulation (Figure 6A). To-date, the study of IL-1β release has been limited to the period of time immediately following inflammasome activation and IL-1β processing. However, using punicalagin, we were now able to study IL-1β secretion independently of inflammasome activation. IL-1β release occurred within the first five minutes after the removal of punicalagin (Figure 6B). This release was paralleled by a decrease of intracellular IL-1β (Figure 6B). Contrary to NLRP3 inflammasome activation, the release mechanism of IL-1β was independent of K^+ efflux or changes in intracellular Ca^{2+} or Na^+ (Figure 6C). The IL-1β release mechanism was also independent of the P2X7 receptor or purinergic signalling, cathepsin or caspase-1 activity (Figure 6C). Metalloprotease inhibition or Zn^{2+} chelation also failed to block IL-1β release (Figure 6C). The activity of apoptotic caspases 3 and 7, phospholipases A and C, autophagy, or tubulin and actin cytoskeleton dynamics, were also not required for the release of IL-1β (Figure 6C). In addition, after washing punicalagin there was a fast membrane permeabilisation and release of LDH (Figure 6D,F), suggesting that IL-1β release

was dependent upon membrane permeabilisation. However, LDH release was mechanistically overlapping with the increase of plasma membrane permeability involved in the release of IL-1β, since treatment of the cells with the cytoprotective agent glycine after washing punicalagin, prevented the release of LDH and the p10 active fragment of caspase-1 from the cell, without affecting the release of mature IL-1β or permeabilisation of the plasma membrane (Figure 6G,H and Supplementary Figure 4E).

Punicalagin prevented phosphatidylserine flip in macrophages after ATP stimulation (Figure 7A), and after punicalagin washout phosphatidylserine was quickly exposed to the outer bilayer (Figure 7A), suggesting its effects were reversible. To further study the effect of punicalagin on plasma membrane fluidity/stability, we labelled cholesterol rich rafts with cholera toxin B-AlexaFluor 647 and followed the dynamics of the rafts over time by quantifying the mean fluorescence intensity in different regions of interest of the plasma membrane. Addition of punicalagin dramatically attenuated the movement of rafts on the plasma membrane (Figure 7B, supplementary movies 6 and 7) and also prevented bleb formation in response to ATP (Figure 7C, supplementary movies 8 and 9). Furthermore, punicalagin was able to impair lipid distribution among plasma membrane using liposomes consisting of fluorescently 549/565 nm (em/ex)-labelled amphipathic molecules (Figure 7D), but it did not impair delivery of fluorescently 480/501 nm (em/ex)-labelled marker particles contained within the lumen of liposomes into the cell cytosol (Figure 7D). Therefore punicalagin stabilizes lipids on the plasma membrane after ATP stimulation, and this lipid stabilization is important for IL-1β release.

Discussion

The vast majority of proteins that are secreted from the cell depend upon a signal peptide at their N-terminus that directs their trafficking into the ER, through which they transit to the Golgi and are then exocytosed from the cell[23]. However, there are a small number of important proteins that lack a signal peptide and do not utilise the ER-Golgi route of protein secretion[24,25]. The secretion of the pro-inflammatory cytokine IL-1β is an enduring question spanning almost 30 years, since the discovery that IL-1β lacks a signal peptide[19] and does not traffic through the ER and Golgi[26]. Despite a number of interesting ideas, all supported by biochemical data, no consensus for a mechanism of IL-1β secretion exists[5]. However, given its contribution to major disease states[27] understanding the mechanisms of IL-1β secretion may allow us to identify new therapeutic targets for the treatment of inflammatory disease.

Despite sharing little sequence homology, IL-1β and the unconventionally secreted protein FGF2 are close structural homologues[10,11]. One of the proposed mechanisms for the secretion of IL-1β has been its direct release across the plasma membrane *via* a mechanism that is closely followed by lysis of the secreting cell[12,28]. Recent evidence using a live single cell assay to measure released IL-1β suggests that changes in membrane permeability are required for its secretion[8]. Recent work has identified that FGF2 is directly secreted across the plasma membrane *via* a mechanism dependent upon its recruitment by the plasma membrane lipid $PI(4,5)P_2$[9,16] and thus it was tempting to speculate that these unconventionally secreted proteins may share a common mechanism of release. However, under the experimental conditions used here it would appear that the mechanisms of IL-1β and FGF2 secretion are distinct, with only FGF2 being able to directly permeabilise membranes in the assays used here. This is not to say, however, that the conditions of these assays did not favour the permeabilising effects of IL-1β, and that different experimental conditions are required. Conventional biochemical methods have limited the investigation into the processes involved in IL-1β secretion to population dynamics, although recent

advances in single cell assays have provided new insights into the dynamics of IL-1β secretion[8]. To further examine the mechanisms of IL-1β secretion we developed a live single cell real time assay for measuring IL-1β release. Immortalised BMDMs transduced to express pro-IL-1β with a C-terminal Venus fluorescent protein tag allowed us to visualise IL-1β secretion using real-time single-cell confocal microscopy. Secretion of IL-1β from these cells after NLRP3 inflammasome activation with ATP appeared normal as assayed by biochemical techniques and the data on IL-1βVenus we recorded was completely consistent with the study of Shirasaki et al.,[8]. The secretion of IL-1βVenus correlated closely with the permeabilisation of the plasma membrane as measured by PI uptake. These data suggest that the secretion of IL-1β from macrophages following inflammasome activation is dependent upon a permeabilisation of the plasma membrane.

We were able to confirm the requirement of plasma membrane permeabilisation using novel membrane stabilising agents that prevented the release of mature IL-1β, but that had no effect on inflammasome assembly and caspase-1 activation. Given the close relationship between IL-1β processing after inflammasome activation and its release[12], interventions that inhibit the release of IL-1β have done so exclusively by blocking inflammasome activation and thus inhibiting its processing to a mature form. We discovered that the complex polyphenolic compound punicalagin is a novel and potent specific inhibitor of the IL-1β release mechanism. These data are the first demonstration of an intervention blocking the release pathway of mature IL-1β in response to different NLRP3 activators. Previous studies on IL-1β release have focused on NLRP3 activation via ATP application and P2X7 receptor signalling[7,8,12,29,30]. Here we report that, in addition to ATP, punicalagin is also able to block mature IL-1β release from macrophages stimulated with nigericin, MSU crystals or hypotonicity, the pore forming toxin melittin and also in response to AIM2 activation *via* dsDNA, pointing to a common mechanism for the release of this cytokine. Entirely consistent with our data on the requirement of membrane permeabilisation, we identified that the mechanism of action for punicalagin appeared to be *via* plasma membrane lipid stabilisation

and consequently inhibition of permeability. Punicalagin did not affect the release of IL-1α, or classically secreted cytokines, such as TNF-α or IL-6. Early events of cell death are characterized by phosphatidylserine exposure to the external plasma membrane bilayer[31], and P2X7 receptor activation results in a fast phosphatidylserine flip to the outer leaflet of the plasma membrane[32]. Here we found that membrane stabilisation by punicalagin affected not only lipid fluidity, but also blocked P2X7 receptor induced phophatidylserine flip and other markers of cell integrity (plasma membrane permeabilisation and LDH leakage), even when active caspase-1 was found intracellularly. Caspase-1 activity is suggested as the main driver of a specific programme of cell death termed pyroptosis which is associated with the leakage of intracellular proteins, including the release of large inflammasome complexes[33,34]. Our data show that both mechanisms, membrane permeability and caspase-1 activity, are important and independent mechanisms leading to IL-1β release from macrophages, with plasma membrane permeability dependent on signal 2 since it was unaffected in caspase-1 deficient macrophages. The specific membrane stabilising effects of punicalagin were rapidly reversible, and following its washout mature IL-1β and the inflammasome components NLRP3, ASC and active caspase-1 were rapidly released. Punicalagin also stabilised the cell membrane to detergents and prevented LDH leaking in response to detergent or NLRP3 inflammasome activation, and furthermore it impaired necroptotic cell death, suggesting it has a broad effect on membrane stabilisation. Pharmacological characterisation of this release pointed to a process independent of caspase-1 activity, but occurred in parallel to the death of the macrophage. When using glycine as a cytoprotective agent[35], we found that after punicalagin washout, glycine was able to impair LDH and caspase-1 release, but did not prevent plasma membrane permeabilisation and IL-1β release. Together these data allow us to propose a model of IL-1β release from macrophages after inflammasome activation which is a non-specific loss of plasma membrane integrity. In cells such as neutrophils, where IL-1β release occurs in the absence of cell death[14], punicalagin also inhibited IL-1β release, indicating a common, albeit

better controlled, secretion mechanism that in macrophages overlaps with cell death. Recently the cytoplasmic protein gasdermin D (Gsdmd) was reported to be critical for membrane permeabilisation and IL-1β release during pyroptosis[36,37]. Gsdmd is a substrate for caspase-1 and -11 and cleavage allows the N-terminal fragment of Gsdmd to destabilise membranes facilitating pyroptosis in both non-canonical and canonical NLRP3 pathways[36-38]. The effects of punicalagin reported here are remarkably similar to the effects of knocking out Gsdmd, in that while release is inhibited, mature caspase-1 and IL-1β are retained inside the cell following NLRP3 activation[37,38]. Whether punicalagin is an inhibitor of Gsdmd cleavage, or of the N-terminal fragment's signalling pathway, or acts independently of Gsdmd, remains to be determined. However, the functional phenotype of Gsdmd knockout, or punicalagin treatment is at present indistinguishable, and this report is the first to describe an intervention of this kind.

Materials and Methods

Reagents

LPS, DAPI (4,6-diamidino-2- phenylindol), ATP, Triton X-100, digitonin, apyrase, TPEN, colchicine, cytochalasin B, 3-methyladenine, U73122, methyl arachidonyl fluoophosphonate, ellagic acid, glycine, and nigericin were from Sigma; Punicalagin ≥ 98% (HPLC) was also from Sigma, but in some experiments an aqueous pomegranate extract produced by Probelte Biotechnology S.L. (Pomanox™) with a content in punicalagin of 20 % (w/w) was used to compare efficacy of the extract with the HPLC purified punicalagin; Punicalin was produced after degradation of punicalagin with tanase (Sigma, 2 U/ml for 8 days), HPLC was used to identify correct punicalagin production; Urolithin A and B were from Kylolab S.L.; BAPTA-AM, E-64, pluronic acid, MMP408, MMP9 inhibitor I, GM 6001, recombinant caspase-1, the caspase-1 inhibitor Ac-YVAD-AOM, the Caspase-3/7 Inhibitor II Ac-DNLD-CHO, the caspase 3 inhibitor I Ac-DEVD-CHO and the specific caspase-1 substrate z-YVAD-AFC were from Merk-Millipore; monosodium urate crystals was from Enzo Life Sciences; A438079 was from Tocris; Yo-Pro-1 iodide, Fura-2 AM, Coelenterazine H, and Cholera Toxin Subunit-Alexa Fluor 647 (CTB-AF647) were from LifeTechnologies; Fuse-It liposomes with 549/565 nm labelled amphipathic molecules within their shell and 480/501 nm labelled marker particles within their lumen were from Ibidi; The general caspase inhibitor Z-VAD-FMK (zVAD) was from Promega; Melittin was synthesized by solid-phase and was a generous gift of Dr. L. Rivas, *Centro Nacional Biotecnología*, Madrid; horseradish peroxidase–anti-β-actin (C4; sc-47778HRP), rabbit polyclonal antibody to caspase-1 p10 (M-20; sc-514), anti-IL-1β (H-153; sc-7884) and anti-ASC ((N-15)-R; sc-22514-R) were from Santa Cruz Biotechnology. Mouse monoclonal anti- NLRP3 (Cryo-2; AG-20B-0014) was from AdipoGen. Secondary antibodies for immunoblot analysis (ECL horseradish peroxidase– conjugated–linked whole sheep antibody to mouse IgG (NA931V) and ECL horseradish peroxidase–conjugated–linked donkey antibody (F(ab′)2 fragment) to rabbit IgG (NA9340V)) were from GE Healthcare.

Membrane binding and pore formation experiments

Expression and purification of recombinant protein: Murine IL-1β variants (mature and pro form) were expressed as recombinant fusion proteins in *Echerichia coli* strain W3110Z1 (18°C for 5h in LB medium) using the expression vectors pQE30 (Qiagen). C-terminal GFP-fusions were expressed in *Echerichia coli* BL21-Codon+ (DE3)-RIL (Stratagene) (18°C for 6h in LB medium) using pET-15b vectors. Expression of FGF2-Y81pCMF was performed as described before[9,16]. All proteins were affinity-purified through a N-terminal His-Tag using standard procedures[9].

Preparation of liposomes[9,16]: All lipids were purchased from Avanti Polar Lipids. Lipid mixtures were first prepared in chloroform, which was evaporated under nitrogen stream. The resulting lipid film was further dried and then resuspended to form liposomes with a final lipid concentration of 4 mM (binding experiments) or 8 mM (carboxyfluorescein dequenching experiments). Unilamellar liposomes were made by 10 freeze/thaw cycles followed by size extrusion through a 400 nm filter for 21 times (Avanti Polar Lipids mini-extruder). Analysis of liposome preparations using dynamic light scattering (Wyatt Technology DynaPro NanoStar) showed a size distribution of 200 to 400 nm in diameter.

Biochemical analysis of protein binding to liposomes: Liposomes with plasma membrane-like lipid composition containing 2 mol % $PI(4,5)P_2$ and phosphatidylcholine liposomes containing 10 mol % $PI(4,5)P_2$ were made as described[15,18]. After incubating mature IL-1β, pro-IL-1β and FGF2-Y81pCMF (5 μM) membranes were reisolated by flotation. Material was analyzed by SDS-PAGE under reducing conditions (loading about 2.25% load and fractions 1-4) followed by Western blotting using anti-IL-1β (antibodies-online GmbH) and anti-FGF2

antibodies, respectively. Signals were acquired using an Odyssey infrared imaging system and quantified using Image Studio Software Version 2.1.10 (LI-COR Bioscience).

Flow cytometry based protein binding to liposomes analysis: Mature IL-1β, pro-IL-1β and FGF2-Y81pCMF (1 µM) were incubated with membranes for 2 h at 25 °C. Protein-bound liposomes were washed by centrifugation (15000 x g; 25°C; 10min). The liposome pellet was resuspended followed by fluorescence-activated cell sorting (FACS) measurements using a FACS Calibur (Becton Dickinson) and data processing using CellQuest Pro software as described[18].

Analysis of membrane pore formation: Membrane pore formation by mature IL-1β, pro-IL-1β and FGF2-Y81pCMF was analysed as described previously[9]. Liposomes with plasma membrane-like lipid composition containing 2 mol % $PI(4,5)P_2$ and phosphatidylcholine liposomes containing 10 mol % $PI(4,5)P_2$ were prepared with 100 µM membrane-impermeant fluorophore 5(6)-carboxyfluorescein (CF Sigma). For removal of extraluminal CF, first liposomes were harvested by centrifugation at 15,000 x g for 10 min at 20 °C, followed by size exclusion chromatography using a PD10 column (GE Healthcare). Afterwards mature IL-1β, pro-IL-1β and FGF2-Y81pCMF (2 µM) were incubated with liposomes and fluorescence dequenching was measured using a SpectraMax GeminiXS fluorescence plate reader (Molecular Devices). At the end of each experiment, Triton X-100 (0.2% (w/v) final concentration) addition enabled to assess maximal dequenching, which was used to normalize data.

Cells and treatments

Immortalised bone marrow derived macrophages (iBMDMs) were transduced by lentivirus to stably express IL-1β tagged with the fluorescent protein Venus (IL-1βVenus). Alternatively, iBMDMs were transiently transfected with IL-1βVenus or HEK293 cells with P2X7 receptor and NLRP3 tagged with YFP and Luciferase using Lipofectamine2000 according to the manufacturer's instructions (Life Technologies). iBMDMs expressing IL-1βVenus or ASC-mCherry[34] were maintained in Dulbecco's modified Eagle's medium (DMEM) supplemented with 10% (heat inactivated) Foetal bovine serum (FBS), 1% (2mM) L-glutamine Q and 1% penicillin-streptomycin. HEK293 cells were maintained in DMEM:F12 (1:1) supplemented with 10% FCS, 2 mM Glutamax and 1% penicillin-streptomycin. Primary BMDMs were obtained from wild type C57BL/6, *Nlrp3*$^{-/-}$ [39] or *Casp1*$^{-/-}$ [40] and differentiated *in vitro* with 20% of L-cell media as reported elsewhere[41]. Mouse neutrophils were isolated from bone marrow using the Mouse Neutrophil Enrichment Kit (StemCell Technologies) according to the manufacturer's instructions. Purity of enriched neutrophils ranged from 73-75% as assessed by flow cytometry with double staining for CD11b (MCA74A488, AbD Serotec) and Ly-6G (clone 1A8, TonboBiosciences). To stimulate the release of IL-1β cells were primed with bacterial endotoxin (LPS, 1 μg/ml for macrophages or 100 ng/ml for neutrophils, 4h – signal 1) and then treated with ATP (5mM, from 0.5 to 1h as stated in figure legends – signal 2) in physiological solution consisting of NaCl (147 mM), HEPES (10 mM), glucose (13 mM), $CaCl_2$ (2 mM), $MgCl_2$ (1 mM), and KCl (2 mM). Alternatively, after LPS-priming cells were stimulated with nigericin (5 μM, 30 min); hypotonic solution (90 mOsm, achieved by diluting the physiological solution 1:4 with distilled sterile water); MSU crystals (200 μg/ml, 16 h); or dsDNA delivered using Lipofectamine2000 (1 μg DNA, 16 h).

Live cell imaging

Cells were plated onto 35mm-glass bottomed dishes (Greiner Bio-One) and incubated on the microscope stage at 37°C in humidified 5% CO_2. For monitoring membrane permeabilisation cells were incubated with propidium iodide (5µg/ml). A Zeiss LSM710 confocal microscope with a Plan-apochromat x63 1.3 NA oil immersion and x40 1.3 NA objectives was used to visualise release of IL-1β. Image capture was performed using the "Zen 2010b SP1" Zeiss software. Alternatively, macrophages were imaged with a Nikon Eclipse Ti microscope equipped with a 40x/0.60 S Plan Fluor objective and a digital Sight DS-QiMc camera (Nikon) and the NIS-Elements AR software (Nikon). Time-lapse microscopy images were quantified either with ImageJ (US National Institutes of Health) or Cell Tracker (version 0.6)[42]. To quantify changes in plasma membrane dynamics over the time, macrophages were labelled with CTB-AF647 (1:1000 dilution) for 30 min at 37ºC and imaged using the Nikon Eclipse Ti microscope as stated above. Inverted fluorescence images converted to grey scale were used for quantification of the mean grey value as relative fluorescence units (RFU) in different regions of interest of the plasma membrane of each cell using ImageJ (US National Institutes of Health).

Fluorescence microscopy

BMDM or immortalized ASC-mCherry macrophages were seeded on coverslips. For phosphatidylserine immunostaining, cells were incubated with Annexin V-FITC (BD Biosciences) for 10 min at room temperature according to the manufacturer's instructions. To study liposome fusion to the plasma membrane, cells were incubated during 120 min at 37ºC with the Fuse-It liposomes (Ibidi), prepared according to manufacturer's instructions. Then cells were fixed with 4% formaldehyde in PBS for 15 min, washed three times with PBS and images were acquired with a Nikon Eclipse Ti microscope as stated above but using a 60x Plan Apo Vc objective (numerical aperture, 1.40) and a Z optical spacing of 0.2

μm. Images were deconvolved using ImageJ software (US National Institutes of Health) with Parallel Iterative Deconvolution plugin, and maximum-intensity projections images are shown in the results.

Fura-2 AM and Yo-Pro uptake assays

Changes in free intracellular calcium concentration were measured with the fluorescent indicator Fura-2 AM. BMDMs were loaded for 40 min at 37ºC with 4 μM Fura-2 AM and 0.02% pluronic acid, washed and fluorescence was recorded by an automatic fluorescence plate reader (Synergy Mx; BioTek) for 200 s at 4 s intervals at a wavelength emission couple 340/380 nm, emission 510 nm. ATP was automatically injected into the wells at the designated time points. Intracellular calcium levels were expressed as the ratio of the emission intensities at 340 and 380 nm, and the value was normalized to the fluorescence at time 0 (F/F_0). For Yo-Pro uptake, BMDMs were preincubated for 10 min at 37 °C with 25 μM of punicalagin, following the addition of 2.5 μM Yo-Pro. The images were recorded at 10 s intervals for 60 min before and during injection at 37 °C with ATP, digitonin or Triton-X100. Yo-Pro bound to DNA fluorescence was measured at 485±9/515±9 nm with bottom excitation/emission in the Synergy Mx plate reader (BioTek). In some experiments Yo-Pro uptake was acquired with a Nikon Eclipse Ti microscope as stated above but using a 20x objective and time-lapse images were analysed with ImageJ software (US National Institutes of Health) and average of relative fluorescence units recorded from ROI are shown in the results.

Western blotting and ELISA

After cells were stimulated, cell supernatants were collected and centrifuged at 300*g* for 8 min at 4°C to remove detached cells and generate a cell-free preparation. Before Western

blot analysis, proteins in supernatants were concentrated by centrifugation at 11,200*g* for 30 min at 4°C through a column with a cut-off of 10 kDa (Microcon; Merk-Millipore). Detailed methods used for cell lysis and Western blot analysis had been described previously[43]. The ELISAs kit for mouse IL-1β, IL-6, TNF-α and IL-1α were from R&D and were used following the manufacturer's instructions.

Bioluminescence resonance energy transfer measurements

Transfected HEK293 cells were plated on a poly-L-lysine–coated 96-well plate; after adhesion, cells were washed with PBS with calcium and magnesium, and readings were performed immediately after the addition of 5 mM coelenterazine-H substrate in physiological solution. Signals were detected with two filter settings (Renilla-luciferase (Luc) filter [485 ± 20 nm] and YFP filter [528 ± 20 nm]) at 37ºC using the Synergy Mx plate reader before and after automatic ATP injection. The bioluminescence resonance energy transfer (BRET) ratio was defined as the difference between the emission at 530 nm/485 nm of R-Luc and YFP NLRP3 fusion protein and the emission at 530 nm/485 nm of the R-Luc fusion NLRP3 alone. Results are expressed in milliBRET units normalized to basal signal.

Lactate dehydrogenase (LDH)–release, Caspase-1 activity and K^+ measurements

The presence of LDH in cell supernatants was measured using the Cytotoxicity Detection kit (Roche), following the manufacturer's instructions. It was expressed as the percentage of the total amount of LDH in the cells. In some control experiments, 25 μM of punicalagin was mixed with a lysate of BMDMs before LDH activity measurement. Caspase-1 activity was measured monitoring the cleavage of the fluorescent substrate z-YVAD-AFC at 400/505 using a Synergy Mx plate reader (BioTek) during 30 min intervals during 6 h. Results are presented as the slope of the relative fluorescence units (RFU)/min. Intracellular K^+ was

quantified from BMDMs cell lysates by indirect potentiometry on a Cobas 6000 with ISE module (Roche).

Statistical analysis

Data are presented as the mean ± SEM from the number of assays indicated (from at least three separate experiments). Data were analysed, using Prism (GraphPad) software, by an unpaired two-tailed Student *t* test to determine the difference between two groups or by one-way ANOVA with the Bonferroni multiple-comparison test to determine the differences among more than two groups.

Acknowledgments

We thank I. Coillin for NLRP3 and Caspase-1 deficient mice; E. Latz for mCherry-ASC iBMDMs; M.C. Baños for both molecular and cellular technical assistance; M. Martínez-Villanueva for intracellular K^+ determination. F. Martín-Sánchez was supported by Sara Borrell post-doctoral grant from Instituto Salud Carlos III (CD12/00523) and P. Paszek holds a BBSRC David Phillips Research Fellowship (BB/I017976/1). This work was supported by grants from Instituto Salud Carlos III-FEDER (EMER07/049, PS09/00120, PS13/00174 to P.P.), European Research Council (ERC-2013-CoG 614578 to P.P.), MRC (MR/K015885/1 to M. White) and BBSRC (BB/K003097/1 to M. White and P. Paszek), the European Union Seventh Framework Programme (FP7/2012-2017, grant agreement n° 305564, to M. White and P. Paszek), the German Research Council (DFG-SFB 638, DFG-SFB/TRR 83, DFG-GRK1188 to WN), the AID-NET program of the Federal Ministry for Education and Research of Germany (to WN) and the DFG cluster of excellence CellNetworks (to WN).

Author Contributions

Execution of experiments: F.M-S., A.B-M., A.I.G., C.D., J.B., D.G.S., M.Z., J.P.S., M.J.D.D.

Punicalagin extract production: M.P.

Analysis and interpretation of data: F.M-S., W.N., D.B., P.P.

Writing of the manuscript: W.N., P.P., D.B.

Design and supervision of this study: D.B., P.P., P.Pa., W.N., A.M., M.R.W.

Conflict of Interest

M.P. is employee of Probelte Biotechnology S.L. The other authors declare no competing financial interests.

References

1 Garlanda, C., Dinarello, C. A. & Mantovani, A. The interleukin-1 family: back to the future. *Immunity* **39**, 1003-1018, doi:10.1016/j.immuni.2013.11.010 (2013).

2 Takeuchi, O. & Akira, S. Pattern recognition receptors and inflammation. *Cell* **140**, 805-820, doi:10.1016/j.cell.2010.01.022 (2010).

3 Latz, E., Xiao, T. S. & Stutz, A. Activation and regulation of the inflammasomes. *Nature reviews. Immunology* **13**, 397-411, doi:10.1038/nri3452 (2013).

4 Cassel, S. L. & Sutterwala, F. S. Sterile inflammatory responses mediated by the NLRP3 inflammasome. *European journal of immunology* **40**, 607-611, doi:10.1002/eji.200940207 (2010).

5 Lopez-Castejon, G. & Brough, D. Understanding the mechanism of IL-1beta secretion. *Cytokine & growth factor reviews* **22**, 189-195, doi:10.1016/j.cytogfr.2011.10.001 (2011).

6 Andrei, C. *et al.* Phospholipases C and A2 control lysosome-mediated IL-1 beta secretion: Implications for inflammatory processes. *Proceedings of the National Academy of Sciences of the United States of America* **101**, 9745-9750, doi:10.1073/pnas.0308558101 (2004).

7 MacKenzie, A. *et al.* Rapid secretion of interleukin-1beta by microvesicle shedding. *Immunity* **15**, 825-835 (2001).

8 Shirasaki, Y. *et al.* Real-time single-cell imaging of protein secretion. *Scientific reports* **4**, 4736, doi:10.1038/srep04736 (2014).

9 Steringer, J. P. *et al.* Phosphatidylinositol 4,5-bisphosphate (PI(4,5)P2)-dependent oligomerization of fibroblast growth factor 2 (FGF2) triggers the formation of a lipidic membrane pore implicated in unconventional secretion. *The Journal of biological chemistry* **287**, 27659-27669, doi:10.1074/jbc.M112.381939 (2012).

10 Priestle, J. P., Schar, H. P. & Grutter, M. G. Crystal structure of the cytokine interleukin-1 beta. *The EMBO journal* **7**, 339-343 (1988).

11 Zhu, X. *et al.* Three-dimensional structures of acidic and basic fibroblast growth factors. *Science* **251**, 90-93 (1991).

12 Brough, D. & Rothwell, N. J. Caspase-1-dependent processing of pro-interleukin-1beta is cytosolic and precedes cell death. *Journal of cell science* **120**, 772-781, doi:10.1242/jcs.03377 (2007).

13 Stoffels, M. *et al.* ATP-Induced IL-1beta Specific Secretion: True Under Stringent Conditions. *Frontiers in immunology* **6**, 54, doi:10.3389/fimmu.2015.00054 (2015).

14 Chen, K. W. *et al.* The neutrophil NLRC4 inflammasome selectively promotes IL-1beta maturation without pyroptosis during acute Salmonella challenge. *Cell reports* **8**, 570-582, doi:10.1016/j.celrep.2014.06.028 (2014).

15 Temmerman, K. *et al.* A direct role for phosphatidylinositol-4,5-bisphosphate in unconventional secretion of fibroblast growth factor 2. *Traffic* **9**, 1204-1217, doi:10.1111/j.1600-0854.2008.00749.x (2008).

16 Müller, H. M. *et al.* Formation of Disulfide Bridges Drives Oligomerization, Membrane Pore Formation and Translocation of Fibroblast Growth Factor 2 to Cell Surfaces. *The Journal of biological chemistry* **Feb 18. pii: jbc.M114.622456. [Epub ahead of print]**, doi:10.1074/jbc.M114.622456 (2015).

17 Ebert, A. D. *et al.* Tec-kinase-mediated phosphorylation of fibroblast growth factor 2 is essential for unconventional secretion. *Traffic* **11**, 813-826, doi:10.1111/j.1600-0854.2010.01059.x (2010).

18 Temmerman, K. & Nickel, W. A novel flow cytometric assay to quantify interactions between proteins and membrane lipids. *Journal of lipid research* **50**, 1245-1254, doi:10.1194/jlr.D800043-JLR200 (2009).

19 Auron, P. E. *et al.* Nucleotide sequence of human monocyte interleukin 1 precursor cDNA. *Proceedings of the National Academy of Sciences of the United States of America* **81**, 7907-7911 (1984).

20 Bauernfeind, F. G. *et al.* Cutting edge: NF-kappaB activating pattern recognition and cytokine receptors license NLRP3 inflammasome activation by regulating NLRP3 expression. *Journal of immunology* **183**, 787-791, doi:10.4049/jimmunol.0901363 (2009).

21 England, H., Summersgill, H. R., Edye, M. E., Rothwell, N. J. & Brough, D. Release of Interleukin-1alpha or Interleukin-1beta Depends on Mechanism of Cell Death. *The Journal of biological chemistry* **289**, 15942-15950, doi:10.1074/jbc.M114.557561 (2014).

22 North, R. A. Molecular physiology of P2X receptors. *Physiological reviews* **82**, 1013-1067, doi:10.1152/physrev.00015.2002 (2002).

23 Rothman, J. E. & Wieland, F. T. Protein sorting by transport vesicles. *Science* **272**, 227-234 (1996).

24 Nickel, W. & Seedorf, M. Unconventional mechanisms of protein transport to the cell surface of eukaryotic cells. *Annual review of cell and developmental biology* **24**, 287-308, doi:10.1146/annurev.cellbio.24.110707.175320 (2008).

25 Nickel, W. & Rabouille, C. Mechanisms of regulated unconventional protein secretion. *Nature reviews. Molecular cell biology* **10**, 148-155, doi:10.1038/nrm2617 (2009).

26 Rubartelli, A., Cozzolino, F., Talio, M. & Sitia, R. A novel secretory pathway for interleukin-1 beta, a protein lacking a signal sequence. *The EMBO journal* **9**, 1503-1510 (1990).

27 Dinarello, C. A., Simon, A. & van der Meer, J. W. Treating inflammation by blocking interleukin-1 in a broad spectrum of diseases. *Nature reviews. Drug discovery* **11**, 633-652, doi:10.1038/nrd3800 (2012).

28 Cullen, S. P., Kearney, C. J., Clancy, D. M. & Martin, S. J. Diverse Activators of the NLRP3 Inflammasome Promote IL-1beta Secretion by Triggering Necrosis. *Cell reports* **11**, 1535-1548, doi:10.1016/j.celrep.2015.05.003 (2015).

29 Qu, Y., Franchi, L., Nunez, G. & Dubyak, G. R. Nonclassical IL-1 beta secretion stimulated by P2X7 receptors is dependent on inflammasome activation and correlated with exosome release in murine macrophages. *Journal of immunology* **179**, 1913-1925 (2007).

30 Andrei, C. *et al.* The secretory route of the leaderless protein interleukin 1beta involves exocytosis of endolysosome-related vesicles. *Molecular biology of the cell* **10**, 1463-1475 (1999).

31 Fadok, V. A. *et al.* A receptor for phosphatidylserine-specific clearance of apoptotic cells. *Nature* **405**, 85-90, doi:10.1038/35011084 (2000).

32 Elliott, J. I. *et al.* Membrane phosphatidylserine distribution as a non-apoptotic signalling mechanism in lymphocytes. *Nature cell biology* **7**, 808-816, doi:10.1038/ncb1279 (2005).

33 Baroja-Mazo, A. *et al.* The NLRP3 inflammasome is released as a particulate danger signal that amplifies the inflammatory response. *Nature immunology* **15**, 738-748, doi:10.1038/ni.2919 (2014).

34 Franklin, B. S. *et al.* The adaptor ASC has extracellular and 'prionoid' activities that propagate inflammation. *Nature immunology* **15**, 727-737, doi:10.1038/ni.2913 (2014).

35 Verhoef, P. A., Kertesy, S. B., Estacion, M., Schilling, W. P. & Dubyak, G. R. Maitotoxin induces biphasic interleukin-1beta secretion and membrane blebbing in murine macrophages. *Molecular pharmacology* **66**, 909-920, doi:10.1124/mol.66.4. (2004).

36 Kayagaki, N. *et al.* Caspase-11 cleaves gasdermin D for non-canonical inflammasome signalling. *Nature* **526**, 666-671, doi:10.1038/nature15541 (2015).

37 Shi, J. *et al.* Cleavage of GSDMD by inflammatory caspases determines pyroptotic cell death. *Nature* **526**, 660-665, doi:10.1038/nature15514 (2015).

38 He, W. T. *et al.* Gasdermin D is an executor of pyroptosis and required for interleukin-1beta secretion. *Cell research* **25**, 1285-1298, doi:10.1038/cr.2015.139 (2015).

39 Martinon, F., Petrilli, V., Mayor, A., Tardivel, A. & Tschopp, J. Gout-associated uric acid crystals activate the NALP3 inflammasome. *Nature* **440**, 237-241, doi:10.1038/nature04516 (2006).

40 Kuida, K. *et al.* Altered cytokine export and apoptosis in mice deficient in interleukin-1 beta converting enzyme. *Science* **267**, 2000-2003 (1995).

41 Barbera-Cremades, M. *et al.* P2X7 receptor-stimulation causes fever via PGE2 and IL-1beta release. *FASEB journal : official publication of the Federation of American Societies for Experimental Biology* **26**, 2951-2962, doi:10.1096/fj.12-205765 (2012).

42 Shen, H. *et al.* Automated tracking of gene expression in individual cells and cell compartments. *Journal of the Royal Society, Interface / the Royal Society* **3**, 787-794, doi:10.1098/rsif.2006.0137 (2006).

43 Compan, V. *et al.* Cell volume regulation modulates NLRP3 inflammasome activation. *Immunity* **37**, 487-500, doi:10.1016/j.immuni.2012.06.013 (2012).

Figure Legends

Figure 1. *Membrane binding and pore formation properties of pro-IL1β, mature IL-1β and phosphomimetic FGF2.* (A-C) Biochemical analysis using liposomes characterized by either a plasma-membrane-like lipid composition (PM) with or without 2 mol% $PI(4,5)P_2$ (panel A) or phosphatidylcholine (PC) liposomes with or without 10 mol% $PI(4,5)P_2$ (panel B). Binding properties of mature IL-1β, pro-IL-1β and FGF2-Y81pCMF were compared. Membrane-bound material (fraction 1) was separated from free proteins (fractions 2-4) by membrane flotation in density gradients. Fractions were analyzed by SDS-PAGE and Western blotting using anti-IL-1β and anti-FGF2 antibodies, respectively. Quantification was done using an Odyssey infrared imaging system (LI-COR Bioscience). The amount of protein found in fraction 1 was quantified as the percentage of the total signal from fractions 1-4 (panel C). Mean values with standard deviations of 3 independent experiments (n=3) are shown. (D) Binding of GFP-tagged variants of mature IL-1β, pro-IL-1β, and FGF2-Y81pCMF to liposomes with various lipid compositions as indicated was examined using an assay based upon flow cytometry. Signals were normalized based on FGF2-Y81pCMF binding to PM liposomes containing $PI(4,5)P_2$ that was set to 100%. Mean values with standard deviations (n=3) are shown. (E-F) Liposomes containing luminal carboxyfluorescein either consisting of a plasma-membrane-like lipid composition (PM) containing $PI(4,5)P_2$ (panel E) or phosphatidylcholine (PC) containing $PI(4,5)P_2$ (panel F) were used to monitor membrane integrity upon incubation with the proteins indicated. Membrane pore formation was detected by the release of carboxyfluorescein than can be measured through dequenching. The results shown are representative for 3 independent experiments.

Figure 2. *Real-time secretion of IL-1β.* Immortalised mouse BMDMs expressing IL-1βVenus were treated with LPS (1μg/ml, 4h). Fluorescence of IL-1βVenus (green) and PI (red) was then observed when were treated with or without ATP (5mM). The panels in (A) show

images of brightfield (upper right quad), Venus (upper left quad), PI (lower left quad) and merged (lower right quad). Shown are images for time 0, 60min, and 150min. Raw fluorescence data from cells labelled 1-4 are shown in (B). The fluorescence traces shown in (C) are from control movies where no ATP was added. Scale bar represents 10μm.

Figure 3. *Punicalagin blocks mature IL-1β release and membrane permeabilisation.* (A) Immunoblot analysis of the processing and release of pro-IL-1β in cell lysates and supernatants of LPS-primed (1μg/ml, 4h) BMDM unstimulated (-) or stimulated (+) for 30 min with ATP (5 mM) in presence (+) or absence (-) of punicalagin (PUN; 25 μM). (B) Kinetics of Yo-Pro uptake in BMDMs treated as in (A). (C) Punicalagin concentration-inhibition curves obtained for IL-1β release and Yo-Pro uptake in BMDMs treated as in (A); Punicalagin IC_{50} values were 3.91 μM and 7.65 μM for IL-1β release and Yo-Pro uptake respectively. (D) Kinetics of Yo-Pro uptake in LPS-primed BMDMs treated with digitonin (50 μM) or triton X-100 (0.1%) in presence or absence of punicalagin (PUN; 25 μM). (E) Percentage of extracellular LDH from BMDM treated as in A or for 30 min with detergents as in D in presence (+) or absence (-) of punicalagin (PUN; 25 μM). **$p < 0.005$; ***$p < 0.001$; ns, not significant ($p>0.05$) difference (ANOVA with Bonferroni's post-test). (F) Punicalagin concentration-inhibition curves obtained for LDH release in BMDMs treated as in (A); Punicalagin IC_{50} was 3.67 μM. (G) Deconvolved images of immortalized macrophages expressing pro-IL-1βVenus and stimulated as in A. Shown are images of Venus fluorescence for time 0 (pre-ATP) and 5 or 20 min after ATP application; see supplementary movies 4 and 5. Scale bar represents 10 μm; arrowheads indicate areas where the fluorescence is leaking from the cell.

Figure 4. *Punicalagin retain mature IL-1β in response to different NLRP3 activators.* (A) IL-1β ELISA in cell lysates (orange bars) or supernatants (black bars) from BMDMs primed with LPS (1 μg/ml, 4 h) followed by no stimulation (-) or stimulation with ATP (5 mM, 30 min), nigericin (10 μm, 30 min), hypotonic solution (90 mOsm, 1h), monosodium urate crystal (MSU; 200 μg/ml, 3h), melittin (5 μM, 30 min), or double stranded DNA (dsDNA; 2 μg/ml, 30 min), in absence or presence of punicalagin (PUN; 25 μM). (B) Extracellular LDH from macrophages treated as in A. (C) IL-1β ELISA in supernatants (white bars) or extracellular LDH (black bars) from mouse bone marrow isolated neutrophils primed with LPS (100 ng/ml, 4 h) followed by no stimulation (-) or stimulation with nigericin (10 μm, 30 min) in absence or presence of punicalagin (PUN; 25 μM). (D) IL-1α ELISA in supernatants (left panel) or extracellular LDH (right panel) from BMDMs primed with LPS (1 μg/ml, 4 h) followed by no stimulation (-) or stimulation (+) with zVAD (100 μM, 20 h) in absence or presence of punicalagin (PUN; 25 μM). (E) TNF-α and IL-6 ELISA in supernatants from BMDMs primed with LPS (1 μg/ml, 4 h), washed and followed by incubation for 30 min in absence or presence of punicalagin (PUN; 25 μM). *$p < 0.05$; ***$p < 0.001$ (Student´s *t*-test).

Figure 5. *Punicalagin does not blocks NLRP3 or caspase-1 activation.* (A) Intracellular Ca^{2+} rise in mouse BMDMs primed with LPS (1 μg/ml, 4h) followed stimulation with ATP (1 mM, added when indicated with an arrow) in the absence or presence of punicalagin (PUN; 25 μM). (B) Relative intracellular K^+ concentration of BMDMs treated as in (A) with ATP for 30 min. (C) Kinetic of net BRET signal for NLRP3 protein expressed in P2X7-HEK293 cells unstimulated or stimulated with ATP (5 mM, added when indicated with an arrow). (D) Average quantification (top) and fluorescence microscopy images (bottom) of immortalized ASC-Cherry macrophages containing ASC specks treated as in B. *n* >400 cells/condition, from 2 independent experiments; bar 20 μm. (E,F) Immunoblot analysis (E) and caspase-1

activity measurements (F) of cell lysate and supernatant of BMDMs treated as in (B); ***p < 0.001; ns, not significant (p>0.05) difference (Student's *t*-test).

Figure 6. *IL-1β release pharmacology.* (A) Immunoblot analysis of cell lysate and supernatant of mouse BMDMs primed with LPS (1 μg/ml, 4h), followed by no stimulation (-) or stimulation (+) with ATP (5 mM, 20 min) in absence (-) or presence (+) of punicalagin (PUN; 25 μM) and then washout (+) or not (-) for 20 min. (B) ELISA of IL-1β of cell lysate and supernatant from BMDMs primed as in A. Measures are taken every 5 min during 30 min of ATP stimulation (5 mM) after priming (black circles) or washout after 30 min stimulation with ATP (5 mM) with punicalagin (PUN; 25 μM) (white circles). (C) Immunoblot analysis of cell lysate and supernatant of BMDMs treated as in A and during washout after ATP+PUN cells where incubated with punicalagin (PUN; 25 μM), in a buffer without Ca^{2+}, high K^+ (150 mM), with $NMDG^+$ (0 mM Na^+), or normal ion buffer with BAPTA-AM (100 μM), E-64 cathepsin inhibitor (50 μM), Ac-YVAD caspase 1 inhibitor (100 μM), A438079 P2X7 antagonist (25 μM), apyrase (3 U/ml), MMP408 (1 μM), MMP9 (0.5 μM) and GM6001 (0.5 μM) metalloprotease inhibitors, TPEN Zn^{2+} chelator (50 μM), colchicine (50 μM) and cytochalasin B (2.5 μg/ml), 3-MA autophagy inhibitor (6 mM), U73122 phospholipase C inhibitor (10 μM), MAFP phospholipase A inhibitor (10 μM), Ac-DNLD or Ac-DEVD caspase-3 inhibitors (100 μM). (D,F) Kinetic of Yo-Pro uptake (D) and percentage of extracellular LDH (F) from macrophages treated as in B. (G) Percentage of extracellular LDH release and ELISA of IL-1β in supernatant from BMDMs treated as in A and during washout after ATP+PUN cells where incubated with punicalagin (PUN; 25 μM) or glycine (5 mM). (H) Yo-Pro uptake in BMDMs treated as in G. ***p < 0.001; **p < 0.01; ns, not significant (p>0.05) difference (ANOVA with Bonferroni multiple-comparison test).

Figure 7. *Punicalagin stabilises plasma membrane lipids.* (A) Deconvolved maximum projection fluorescence images of representative BMDMs primed with LPS (1 μg/ml, 4 h), followed by no stimulation (vehicle) or stimulation with ATP (3 mM) for 5 min in absence or presence of punicalagin (PUN, 25 μm) and then labelled with FITC-annexin V. Nuclei stained with DAPI (blue); scale bar represents 20 μm. (B) Mean of relative fluorescence units (RFU) quantification in different regions of interest of the plasma membrane, as indicated in the images inserted, of macrophages primed with LPS as in (A) and then labelled with cholera toxin B-Alexa fluor 647 (CTB), untreated (vehicle, black trace) or treated with punicalagin (PUN, 25 μm, red trace) from the time indicated with an arrow. Movements of stained cholesterol rich patches with CTB results in variations of RFU on the selected ROI, punicalagin prevented these movements; see supplementary movies 6 and 7. (C) Deconvolved images of representative BMDMs stimulated as in A, but with 5 mM of ATP and stained with CTB; Shown are images of CTB fluorescence for time 0 (pre-ATP) and 20 min after ATP application; see supplementary movies 8 and 9. Scale bar represents 10 μm. (D) Deconvolved maximum projection fluorescence images of representative BMDMs primed with LPS as in (A) and incubated for 2 h with the Fuse-It liposomes in absence or presence of punicalagin. Cells are visualized with red-labelled membranes, green-labelled cell lumen and nuclei counterstained with DAPI (blue). Scale bar represent 10 μm, cellular edges are shown with a white dotted line.

Supplementary Figure Legends

Supplementary Figure 1: *Establishment of IL-1βVenus expressing cells.* Immortalised BMDMs were transduced by lentivirus to express pro-IL-1βVenus. Shown is a bright-field image of the BMDMs in culture and the corresponding fluorescence image showing the sub-cellular distribution of the pro-IL-1βVenus (A). Scale bar represents 20μm. These BMDM-IL-1Venus cells were treated plus or minus with LPS (1μg/ml, 4h) and then with the ATP (5mM, 1h). Supernatants were collected and blotted for IL-1β. As seen in panel (B) secretion of tagged or endogenous IL-1β requires LPS priming. The band at 58kDa is pro-IL-1βVenus, at 44kDa is IL-1βVenus, at 31kDa is endogenous pro-IL-1β, and at 17kDa is endogenous IL-1β. These data confirm that the transduced cells are competent for inflammasome activation. WT (i) or IL-1βVenus expressing cells (ii) were treated with LPS (1μg/ml, 4h) and then ATP (5mM) for 10, 20, 30 or 60min with supernatants analysed for IL-1β (C) and LDH (D). Data are the Mean ± SEM, ELISA n=4, LDH n=3.

Supplementary Figure 2: *Punicalagin structure necessary to prevent IL-1β release.* (A) Structure of punicalagin molecule and their component parts punicalin, ellagic acid and urolithin. (B) Immunoblot analysis of the processing of pro-IL-1β in cell lysate and supernatant of BMDMs primed with LPS (1 μg/ml, 4h) and unstimulated (-) or stimulated (+) with ATP (5 mM, 30 min) in absence (-) or presence (+) of punicalagin (PUN; 25 μM), Punicalin (25 μM), Ellagic acid (100 μM), Urolithin A (100 μM) or Urolithin B (100 μM). (C) Immunoblot analysis of IL-1β processing in BMDMs treated as in A but in absence (-) or presence (+) of Pomanox^{TM} as a source of punicalagin at 25 μM.

Supplementary Figure 3: *Punicalagin maintain cell integrity after detergent treatment.* (A) Representative images of BMDMs primed with LPS (1 μg/ml, 4h) and then treated with digitonin (50 μM, 30 min) in absence or presence or punicalagin (25 μM). (B) Percentage of

extracellular LDH release in supernatant from BMDMs treated as in A but with increasing doses of digitonin. (C) Yo-Pro-1 fluorescence on BMDMs primed with LPS (1 μg/ml, 4h) and then treated with ATP (5 mM, 30 min) to obtain maximum fluorescence. Then cells were incubated or not with punicalagin (PUN; 25 μM), and fluorescence signal was excited and recorded from the bottom of the plate. (D) LDH activity measured in BMDM cell lysates incubated or not with punicalagin (PUN; 25 μM), punicalagin did not interfere with LDH enzymatic assay. (E) IL-1βVenus fluorescence quantification in iBMDMs expressing pro-IL-1βVenus primed with LPS (1 μg/ml, 4h) and then untreated (blue trace) or treated with ATP (5 mM, 25 min) in absence (black traces) or presence or punicalagin (25 μM; +PUN, red traces). Each trace represents one independent cell recorded in different days. The cells measured correspond with the cells shown in Supplementary movies 4 and 5.

Supplementary Figure 4: *ELISA validation for mature IL-1β*. (A) Immunoblot analysis (left) and ELISA (right) of the same cell lysate samples from BMDMs primed with LPS (1 μg/ml, 4h) and unstimulated (-) or stimulated (+) with ATP (5 mM, 30 min) in absence (-) or presence (+) of punicalagin (PUN; 25 μM). (B) Volume changes of THP-1 macrophages treated with a hypotonic solution (90 mOsm) in the absence or presence of punicalagin (PUN; 25 μM). (C,D) Kinetic of Yo-Pro uptake (C) and percentage of extracellular LDH and ELISA of IL-1β (D) released from wild-type (WT), *Casp1*$^{-/-}$*Casp11*$^{-/-}$ and *Nlrp3*$^{-/-}$ BMDMs primed with LPS (1 μg/ml, 4h) followed stimulation with ATP (1 mM, added when indicated with an arrow in C) in the absence or presence of punicalagin (PUN; 25 μM). (E) Immunoblot analysis for IL-1β and p10 fragment of active caspase-1 of cell lysate and supernatant of mouse BMDMs primed with LPS (1 μg/ml, 4h), followed by no stimulation (-) or stimulation (+) with ATP (5 mM, 20 min) and punicalagin (PUN; 25 μM), then the cells were washed and incubated for further 20 min in the absence or presence of PUN or glycine (5 mM). ***$p < 0.001$; ns, not significant ($p>0.05$) difference (Student's *t*-test).

Supplementary movie 1: Immortalised mouse BMDMs expressing IL-1βVenus were treated with LPS (1μg/ml, 4h) and imaged using a Zeiss LSM710 confocal microscope. Fluorescence of IL-1βVenus (green) and PI (red) was then observed when were treated with or without ATP (5mM). Image capture was performed using the "Zen 2010b SP1" Zeiss software. The panels in (A) show images of brightfield (upper right quad), Venus (upper left quad), PI (lower left quad) and merged (lower right quad).

Supplementary movie 2: Immortalised mouse BMDMs expressing IL-1βVenus were treated with LPS (1μg/ml, 4h) and imaged using a Zeiss LSM710 confocal microscope. Fluorescence of IL-1βVenus (green) and PI (red) was then observed when were treated with or without ATP (5mM). Image capture was performed using the "Zen 2010b SP1" Zeiss software. The panels in (A) show images of brightfield (upper right quad), Venus (upper left quad), PI (lower left quad) and merged (lower right quad).

Supplementary movie 3: Immortalised mouse BMDMs expressing IL-1βVenus were treated with LPS (1μg/ml, 4h) and imaged using a Zeiss LSM710 confocal microscope. Fluorescence of IL-1βVenus (green) and PI (red) was then observed. Image capture was performed using the "Zen 2010b SP1" Zeiss software. The panels in (A) show images of brightfield (upper right quad), Venus (upper left quad), PI (lower left quad) and merged (lower right quad).

Supplementary movie 4: Time-lapse fluorescence microscopy of iBMDMs expressing pro-IL-1βVenus primed with LPS (1 μg/ml, 4 h) and stimulated with ATP (5 mM). Frames are recorded every 30 sec during 30 min. Monochromatic deconvolved images are shown. Time

(min) is presented as a counter inside the movie. Addition of different treatments is also indicated in the movie. Scale bar represent 10 μm.

Supplementary movie 5: Time-lapse fluorescence microscopy of iBMDMs expressing pro-IL-1βVenus primed with LPS (1 μg/ml, 4 h) and incubated with punicalagin (25 μM) 20 min before and during ATP (5 mM) stimulation. Frames are recorded every 30 sec during 30 min. Monochromatic deconvolved images are shown. Time (min) is presented as a counter inside the movie. Addition of different treatments is also indicated in the movie (punicalagin addition is marked as PB02). Scale bar represent 10 μm.

Supplementary movie 6: Time-lapse fluorescence microscopy of BMDMs primed with LPS (1 μg/ml, 4 h), labelled with cholera toxin B-Alexa fluor 647 and then recorded every 30 sec during 60 min. Monochromatic inverted images are shown. Time (min) is presented as a counter inside the movie. Scale bar represent 10 μm.

Supplementary movie 7: Time-lapse fluorescence microscopy of BMDMs primed with LPS (1 μg/ml, 4 h), labelled with cholera toxin B-Alexa fluor 647 and then recorded every 30 sec during 60 min. Punicalagin (PB02; 25 μM) was added after 7 min of recording and is indicated in the movie as PB02. Monochromatic inverted images are shown. Time (min) is presented as a counter inside the movie. Scale bar represent 10 μm.

Supplementary movie 8: Time-lapse fluorescence microscopy of BMDMs primed with LPS (1 μg/ml, 4 h), labelled with cholera toxin B-Alexa fluor 647 and then recorded every 30 sec during 35 min. ATP (5 mM) was added after 12 min of recording and is indicated in the

movie. Monochromatic inverted images are shown. Time (min) is presented as a counter inside the movie. Scale bar represent 10 μm.

Supplementary movie 9: Time-lapse fluorescence microscopy of BMDMs primed with LPS (1 μg/ml, 4 h), labelled with cholera toxin B-Alexa fluor 647 and then recorded every 30 sec during 35 min. Punicalagin (25 μM; marked as PB02 in the movie) was added after 7 min of recording and ATP (5 mM) after 12 min and both events are indicated in the movie. Monochromatic inverted images are shown. Time (min) is presented as a counter inside the movie. Scale bar represent 10 μm.

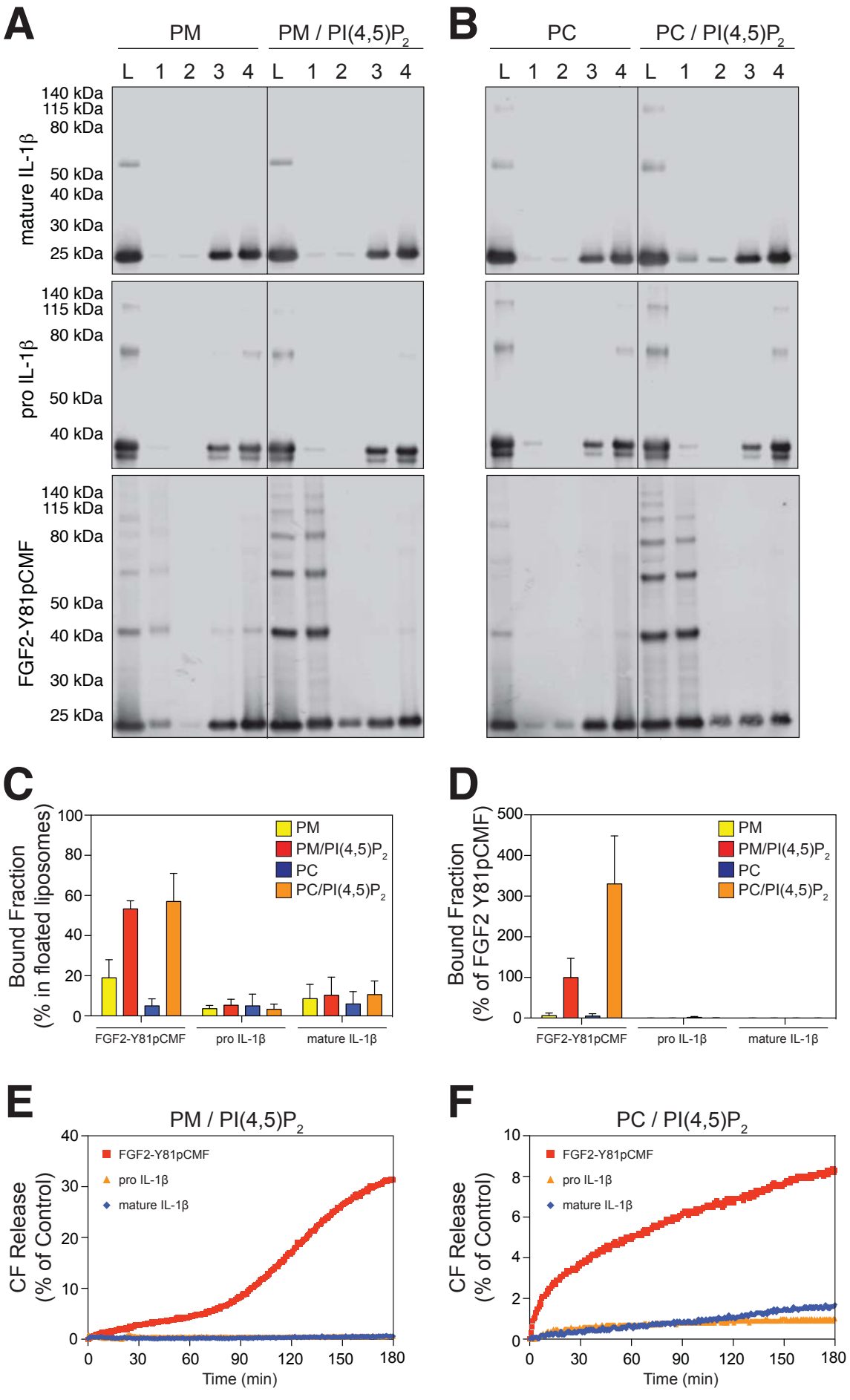
A
PM
PM / PI(4,5)P2
L 1 2 3 4 L 1 2 3 4
mature IL-1β
pro IL-1β
FGF2-Y81pCMF
140 kDa
115 kDa
80 kDa
50 kDa
40 kDa
30 kDa
25 kDa
B
PC
PC / PI(4,5)P2
C
Bound Fraction
(% in floated liposomes)
PM
PM/PI(4,5)P2
PC
PC/PI(4,5)P2
FGF2-Y81pCMF
pro IL-1β
mature IL-1β
D
Bound Fraction
(% of FGF2 Y81pCMF)
E
PM / PI(4,5)P2
CF Release
(% of Control)
FGF2-Y81pCMF
pro IL-1β
mature IL-1β
Time (min)
F
PC / PI(4,5)P2

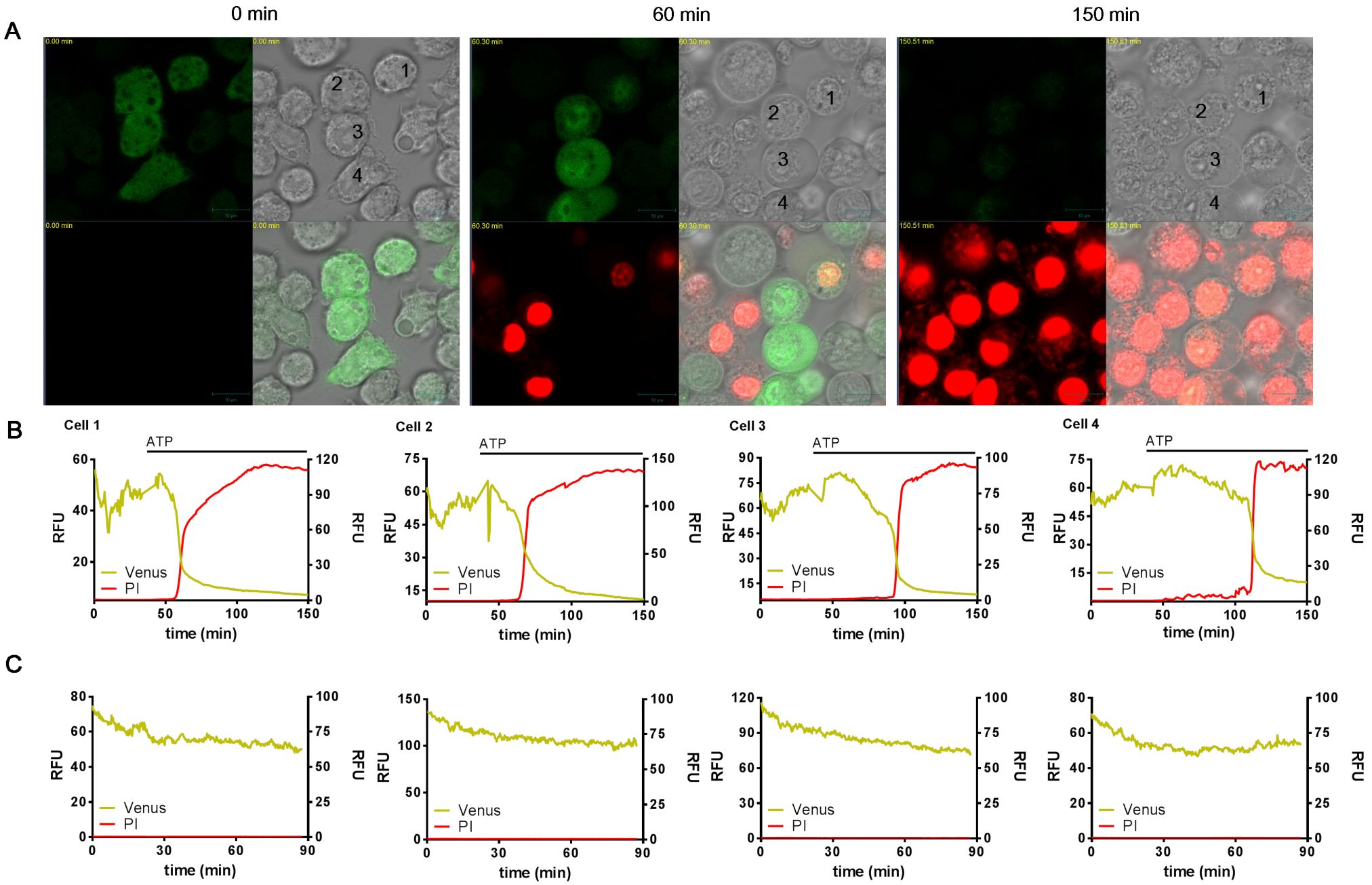
A
0 min
60 min
150 min
1
2
3
4
B
Cell 1
Cell 2
Cell 3
Cell 4
ATP
RFU
Venus
PI
time (min)
C
RFU
Venus
PI
time (min)

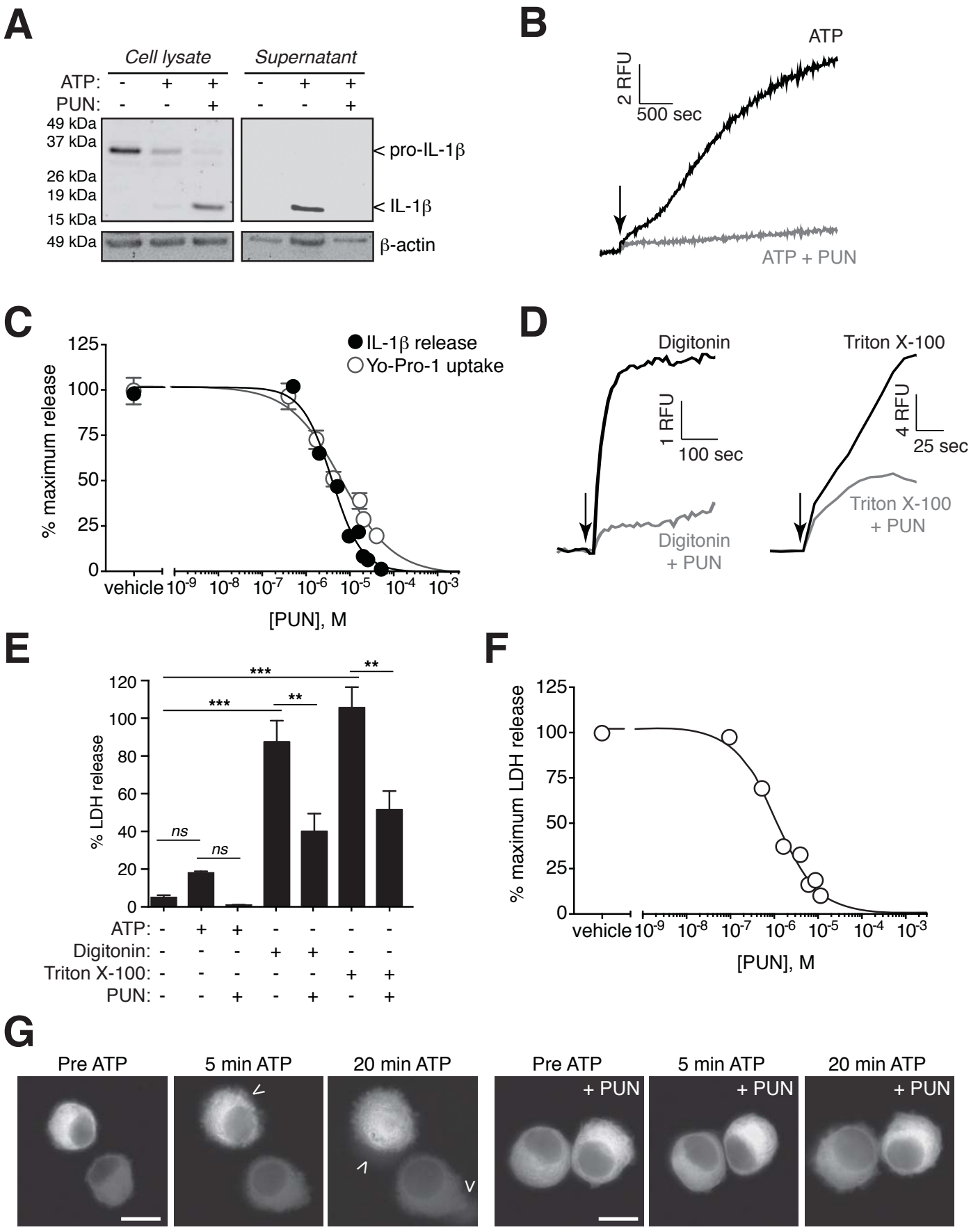
A
Cell lysate
Supernatant
ATP:
PUN:
49 kDa
37 kDa
26 kDa
19 kDa
15 kDa
49 kDa
pro-IL-1β
IL-1β
β-actin
B
ATP
2 RFU
500 sec
ATP + PUN
C
IL-1β release
Yo-Pro-1 uptake
% maximum release
vehicle
[PUN], M
D
Digitonin
1 RFU
100 sec
Digitonin + PUN
Triton X-100
4 RFU
25 sec
Triton X-100 + PUN
E
% LDH release
ns
ns
ATP:
Digitonin:
Triton X-100:
PUN:
F
% maximum LDH release
vehicle
[PUN], M
G
Pre ATP
5 min ATP
20 min ATP
Pre ATP + PUN
5 min ATP + PUN
20 min ATP + PUN

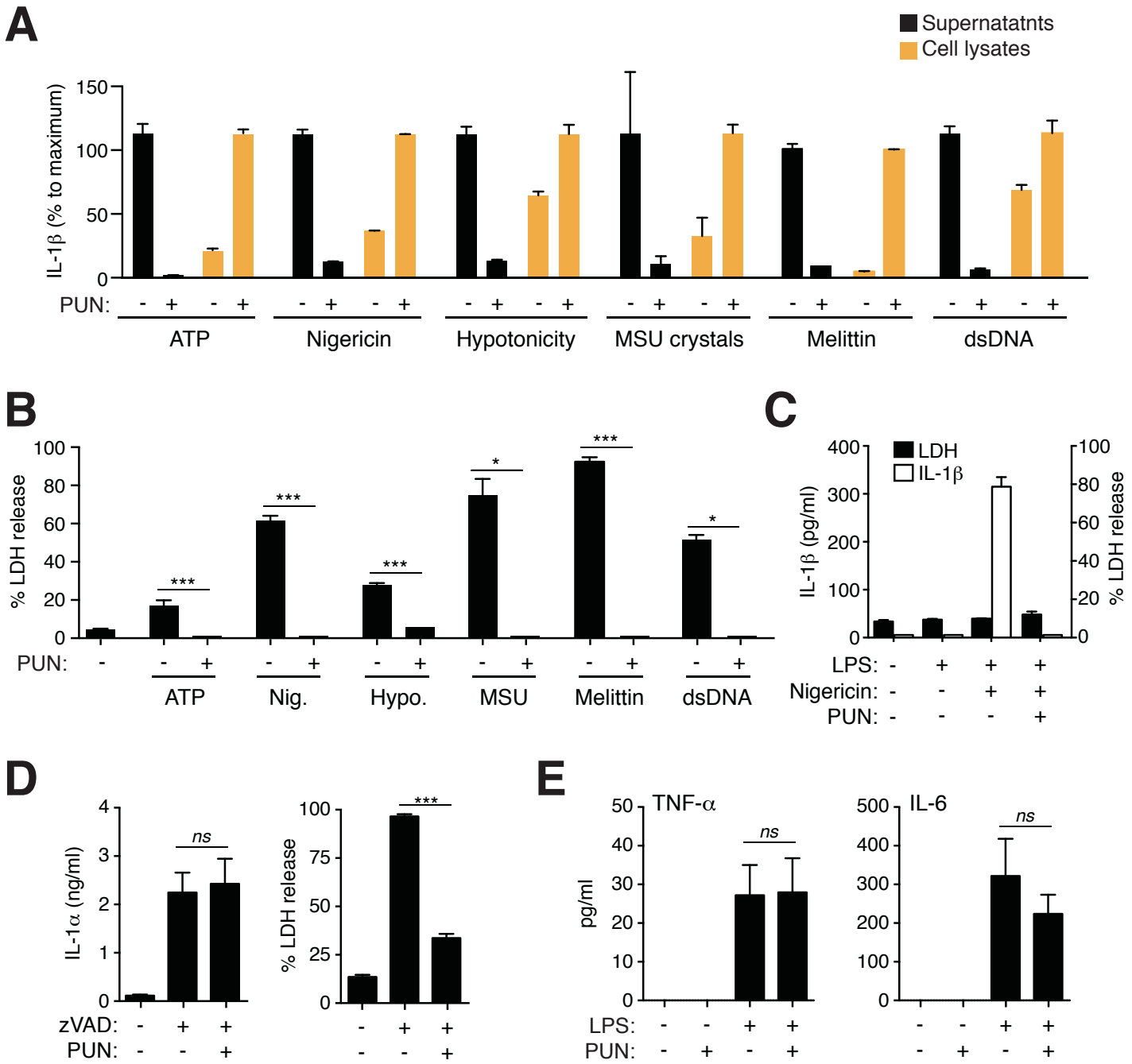
A
Supernatatnts
Cell lysates
IL-1β (% to maximum)
150
100
50
0
PUN: - + - + - + - + - + - + - + - + - + - + - + - +
ATP
Nigericin
Hypotonicity
MSU crystals
Melittin
dsDNA
B
% LDH release
100
80
60
40
20
0
***
***
***
*
***
*
PUN: - - + - + - + - + - + - +
ATP
Nig.
Hypo.
MSU
Melittin
dsDNA
C
LDH
IL-1β
IL-1β (pg/ml)
400
300
200
100
0
% LDH release
100
80
60
40
20
0
LPS: - + + +
Nigericin: - - + +
PUN: - - - +
D
IL-1α (ng/ml)
4
3
2
1
0
ns
% LDH release
100
75
50
25
0
***
zVAD: - + +
PUN: - - +
- + +
- - +
E
TNF-α
pg/ml
50
40
30
20
10
0
ns
IL-6
500
400
300
200
100
0
ns
LPS: - - + +
PUN: - + - +
- - + +
- + - +

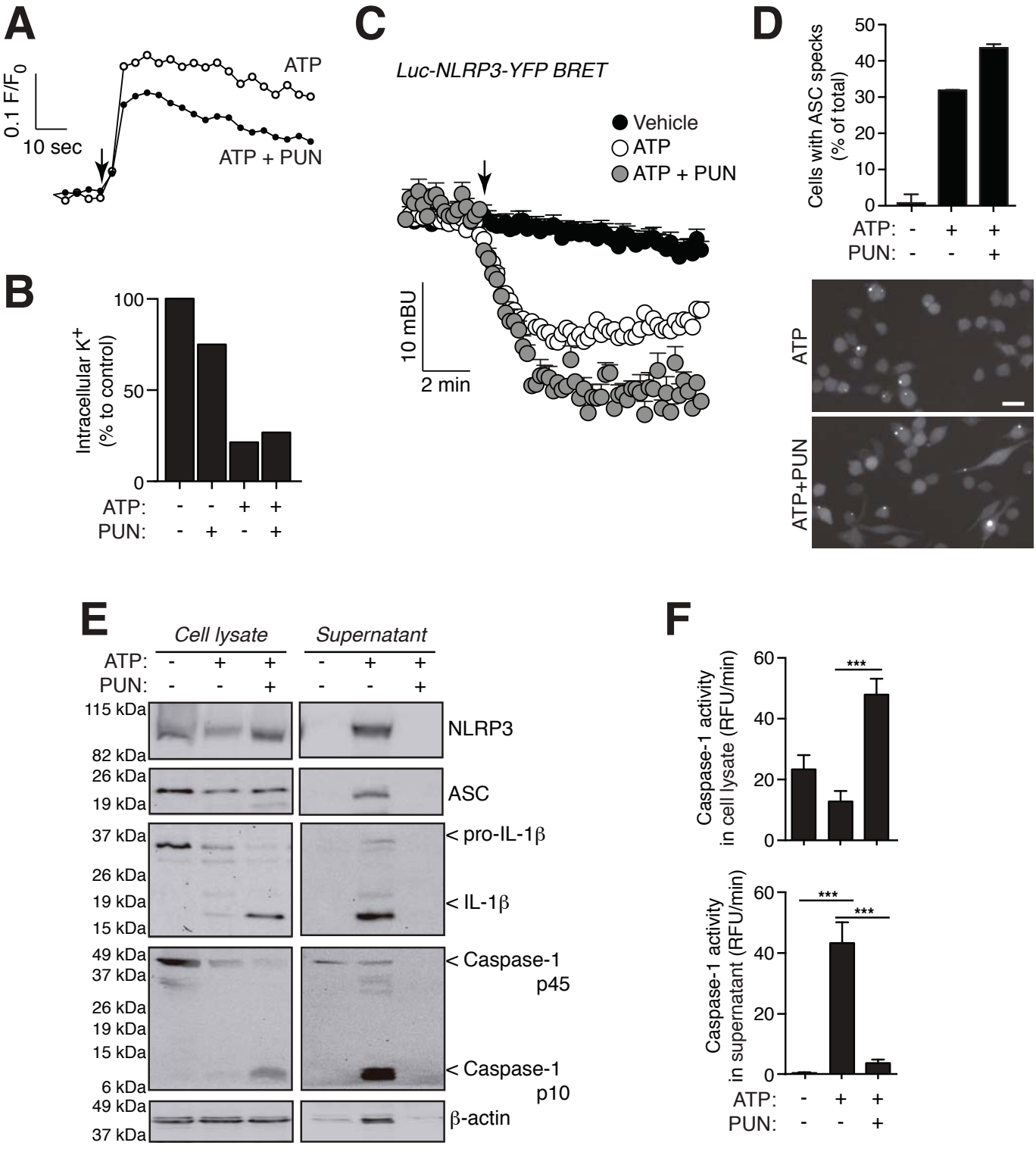
A
0.1 F/F0
10 sec
ATP
ATP + PUN
B
Intracellular K+ (% to control)
100
50
0
ATP: - - + +
PUN: - + - +
C
Luc-NLRP3-YFP BRET
Vehicle
ATP
ATP + PUN
10 mBU
2 min
D
Cells with ASC specks (% of total)
50
40
30
20
10
0
ATP: - + +
PUN: - - +
ATP
ATP+PUN
E
Cell lysate
Supernatant
ATP: - + + - + +
PUN: - - + - - +
115 kDa
82 kDa
NLRP3
26 kDa
19 kDa
ASC
37 kDa
26 kDa
19 kDa
15 kDa
< pro-IL-1β
< IL-1β
49 kDa
37 kDa
26 kDa
19 kDa
15 kDa
6 kDa
< Caspase-1 p45
< Caspase-1 p10
49 kDa
37 kDa
β-actin
F
Caspase-1 activity in cell lysate (RFU/min)
60
40
20
0
***
Caspase-1 activity in supernatant (RFU/min)
60
40
20
0
***
***
ATP: - + +
PUN: - - +

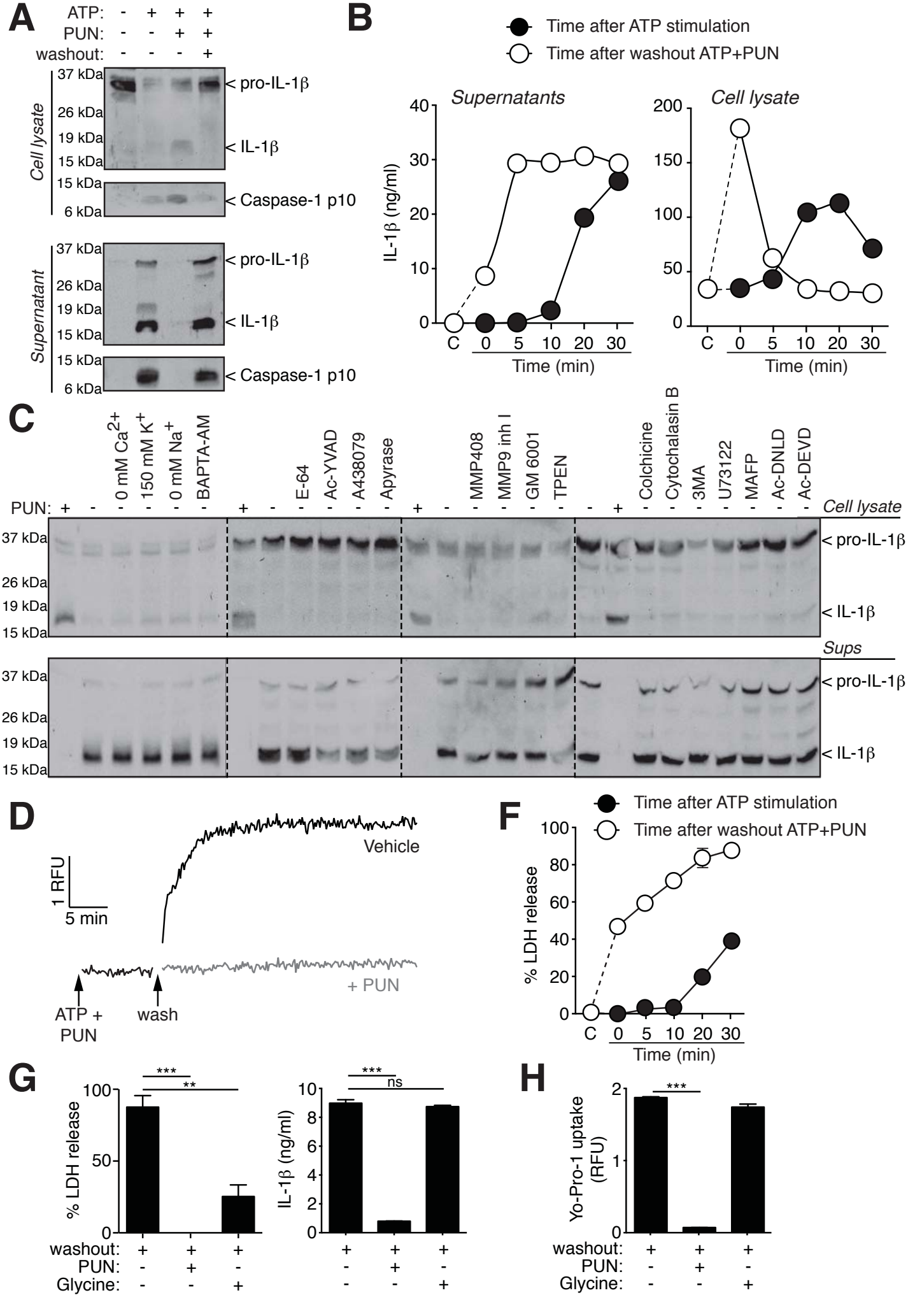
A
ATP: - + + +
PUN: - - + +
washout: - - - +
Cell lysate
37 kDa
26 kDa
19 kDa
15 kDa
< pro-IL-1β
< IL-1β
15 kDa
6 kDa
< Caspase-1 p10
Supernatant
37 kDa
26 kDa
19 kDa
15 kDa
< pro-IL-1β
< IL-1β
15 kDa
6 kDa
< Caspase-1 p10
B
Time after ATP stimulation
Time after washout ATP+PUN
Supernatants
Cell lysate
IL-1β (ng/ml)
40
30
20
10
0
200
150
100
50
0
C 0 5 10 20 30
Time (min)
C
0 mM Ca2+
150 mM K+
0 mM Na+
BAPTA-AM
E-64
Ac-YVAD
A438079
Apyrase
MMP408
MMP9 inh I
GM 6001
TPEN
Colchicine
Cytochalasin B
3MA
U73122
MAFP
Ac-DNLD
Ac-DEVD
PUN: + - + - + - + - + - + - + - + - + - + - + - + - + - + -
Cell lysate
37 kDa
26 kDa
19 kDa
15 kDa
< pro-IL-1β
< IL-1β
Sups
37 kDa
26 kDa
19 kDa
15 kDa
< pro-IL-1β
< IL-1β
D
1 RFU
5 min
Vehicle
+ PUN
ATP + PUN
wash
F
Time after ATP stimulation
Time after washout ATP+PUN
% LDH release
100
80
60
40
20
0
C 0 5 10 20 30
Time (min)
G
% LDH release
100
50
0
***
**
IL-1β (ng/ml)
10
8
6
4
2
0
***
ns
washout: + + +
PUN: - + -
Glycine: - - +
H
Yo-Pro-1 uptake (RFU)
2
1
0
***
washout: + + +
PUN: - + -
Glycine: - - +

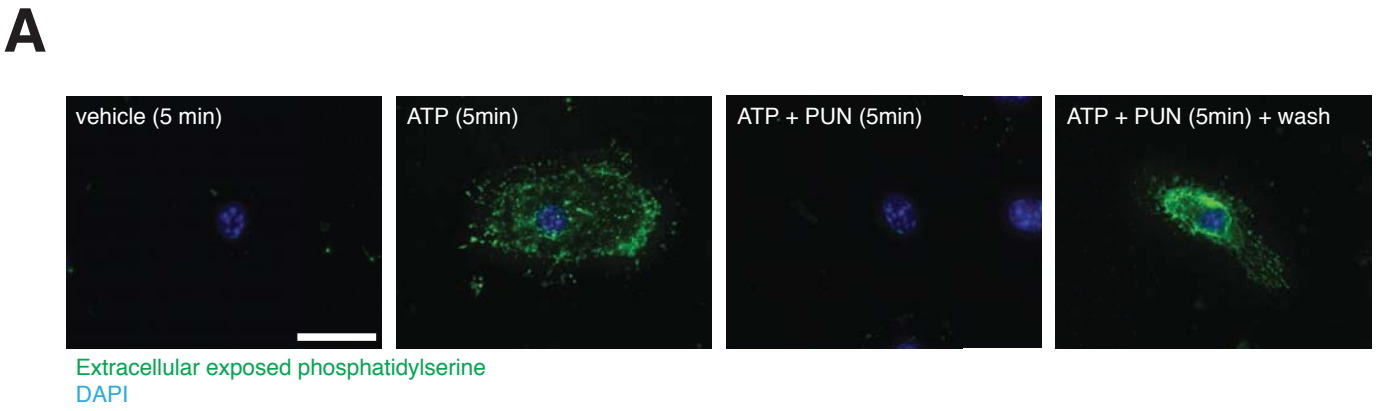
A
vehicle (5 min)
ATP (5min)
ATP + PUN (5min)
ATP + PUN (5min) + wash
Extracellular exposed phosphatidylserine
DAPI
B
5 RFU
10 min
+ vehicle
+ PUN
+ vehicle t=0 min
+ vehicle t=25 min
+ PUN t=0 min
+ PUN t=25 min
C
no treatment
+ punicalagin
pre-ATP
20 min after-ATP
D
549/565 nm (ex/em) lipids
480/501 nm (ex/em) particles
merge + DAPI
no treatment
+ punicalagin